

Table I. Pseudo-First-Order Rate Constants for Reaction of  $\text{Mn}(\text{CO})_3\text{L}_2\cdot$  Radicals with CO at 20 °C

$10^3[\text{CO}], \text{M}$	$[\text{L}], \text{M}$	$k_{\text{obsd}} \text{ s}^{-1}$
	$\text{Mn}(\text{CO})_3[\text{P}(i\text{-Bu})_3]_2\cdot$	
5.0	$<10^{-4}$	$1.6 \times 10^{-3}$
2.5	$<10^{-4}$	$7.9 \times 10^{-4}$
1.7	$<10^{-4}$	$5.2 \times 10^{-4}$
5.0	$5 \times 10^{-3}$	$1.4 \times 10^{-3}$
5.0	$5 \times 10^{-2}$	$1.5 \times 10^{-3}$
	$\text{Mn}(\text{CO})_3[\text{P}(n\text{-Bu})_3]_2\cdot$	
5.0	$\sim 10^{-3}$	$2.1 \times 10^{-1}$

are strongly indicative of an associative pathway. The substituted radicals are thus much less labile than  $\text{Mn}(\text{CO})_5\cdot$ , for which the rate constant for thermal loss of CO is estimated to be in the range  $10\text{--}100 \text{ s}^{-1}$ .<sup>7,9</sup> We had earlier inferred that  $\text{Mn}(\text{CO})_4\text{L}\cdot$  radicals are less labile than  $\text{Mn}(\text{CO})_5\cdot$ .<sup>13</sup> Since observation of an associative process places an upper limit on the possible value for the dissociative loss of CO or L, we can infer an order of labilities  $\text{Mn}(\text{CO})_5\cdot > \text{Mn}(\text{CO})_4\text{L}\cdot > \text{Mn}(\text{CO})_3\text{L}_2\cdot$ .

$\text{Mn}(\text{CO})_3[\text{P}(i\text{-Bu})_3]_2\cdot$  enriched with  $^{13}\text{C}$  was reacted with normal isotopic abundance CO. From the relative rates of disappearance of the IR bands associated with the normal-abundance and  $^{13}\text{C}$ -enriched species it can be inferred that replacement of  $^{13}\text{C}$  by normal-abundance CO occurs at a rate comparable to that for substitution of the phosphine by CO. At this point it is not possible to say whether the replacement of CO by CO occurs via a dissociative or associative process; however, the latter seems more likely. The details of these kinetics studies will be reported later.

The present results, taken together with the results of previous studies, point toward the manner in which replacement of CO by more strongly  $\sigma$ -donating and weaker  $\pi$ -acid phosphines leads to a decreased lability of the metal center. The new observations are consistent with the hypothesis that there may be a transition in the prevalent pathway for substitution, from dissociative for  $\text{Mn}(\text{CO})_5\cdot$  to associative for  $\text{Mn}(\text{CO})_3\text{L}_2\cdot$  radicals. Clearly, however, much remains to be learned about how the choice of metal and attendant ligands affects lability in the radicals.

**Registry No.**  $\text{Mn}(\text{CO})_3[\text{P}(i\text{-Bu})_3]_2\cdot$ , 81971-50-8;  $\text{Mn}(\text{CO})_3[\text{P}(n\text{-Bu})_3]_2\cdot$ , 67551-64-8; CO, 630-08-0.

### Carbon-13 NMR Subspectra of a Protein Based on the Number of Attached Protons. Ferredoxin from *Anabaena variabilis*

Tze-Ming Chan, William M. Westler, Robert E. Santini, and John L. Markley\*

Department of Chemistry, Purdue University  
West Lafayette, Indiana 47907

Received February 8, 1982

The usefulness of  $J$ -modulated spin-echo pulse sequences in the determination of spin multiplicities of  $^1\text{H}$  NMR peaks in proteins was reported several years ago.<sup>1</sup> Recently, an analogous procedure was described for the determination of spin multiplicities in  $^{13}\text{C}$  NMR spectra of small organic molecules.<sup>2,3</sup> We now apply this procedure, which has been given the acronym APT for "attached proton test",<sup>3</sup> to determine the spin multiplicity of peaks in the aromatic region of the  $^{13}\text{C}$  NMR spectrum of a 2Fe-2S\* ferredoxin, a small protein ( $M_r = 11\ 000$ ) involved in photosynthetic electron transport.<sup>4</sup> The APT approach is superior to other

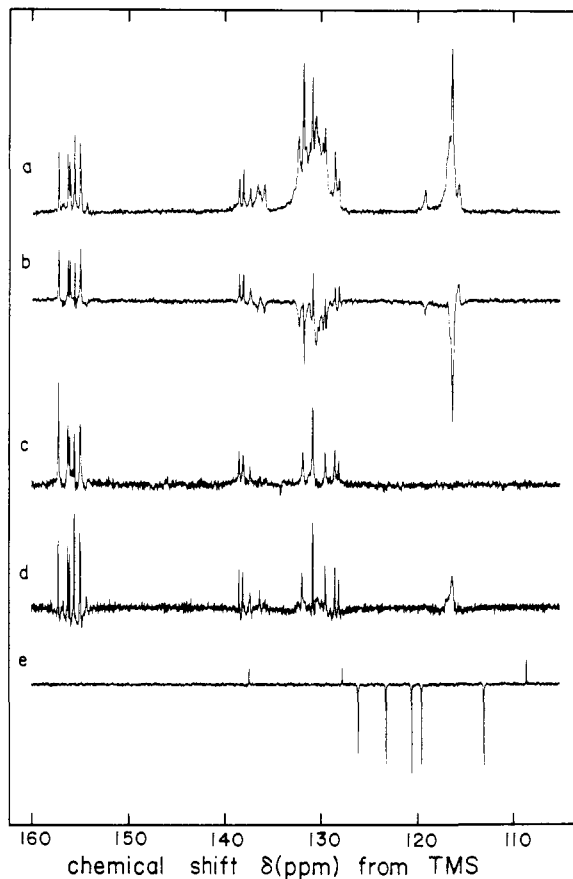


**Figure 1.** Comparison of different strategies used to obtain 50.31-MHz  $^{13}\text{C}$  NMR spectra of the aromatic region of a protein, oxidized ferredoxin from *Anabaena variabilis*.<sup>17</sup> (a) normal, single-pulse experiment with on-resonance broad-band square-wave-modulated  $^1\text{H}$  decoupling; (b)  $J$ -modulated spin-echo pulse sequence with on-resonance, square-wave-modulated  $^1\text{H}$  decoupling<sup>2</sup> (APT experiment);<sup>3</sup> (c) spin-echo spectrum with off-resonance, square-wave-modulated  $^1\text{H}$  decoupling;<sup>12</sup> (d) convolution difference spectrum obtained from a noise-modulated, off-resonance  $^1\text{H}$  decoupled spectrum by subtracting a digitally broadened spectrum from the original;<sup>11</sup> (e) the  $J$ -modulated spin-echo (APT) spectrum of tryptophan, an aromatic amino acid not present in *A. variabilis* ferredoxin, presented for reference purposes.

methods that have been used to determine  $^{13}\text{C}$  NMR multiplicities in proteins; and it is preferable in some cases to a two-dimensional heteronuclear  $J$ -resolved  $^{13}\text{C}$  NMR spectrum in that it provides about the same level of information in much less time. Since the aromatic region contains resonances of carbons with either zero or one attached proton, subspectra containing resonances only of unprotonated or singly protonated carbons can be generated from the sum and difference of the APT spectrum and a normal, noise-decoupled, single-pulse spectrum.

Ferredoxin was isolated from *Anabaena variabilis* grown on  $\text{CO}_2$  [20%  $^{13}\text{C}$ ] as the sole carbon source by a modification of the procedure of Ho et al.<sup>5</sup> The  $^{13}\text{C}$  enrichment level is well above the  $^{13}\text{C}$  natural abundance of 1.1% but below the level at which  $^{13}\text{C}$ - $^{13}\text{C}$  coupling of labeled neighboring carbons complicates the spectra.<sup>6</sup>

The  $^{13}\text{C}$  resonances expected between 110 and 160 ppm arise from the ring carbons of five tyrosines, three phenylalanines, and two histidines, and from the guanidinyll carbon of one arginine present in the sequence of *A. variabilis* ferredoxin.<sup>7</sup> With neglect of long-range couplings which are characterized by small coupling

(1) Campbell, I. D.; Dobson, C. M.; Williams, R. J. P.; Wright, P. E. *FEBS Lett.* **1975**, *57*, 96-99.

(2) Anet, F. A. L.; Jaffer, N.; Strouse, J. *21st Experimental NMR Conference*, 1980. Le Cocq, C.; Lallemand, J.-Y. *J. Chem. Soc., Chem. Commun.* **1981**, 150-152. Rabenstein, D. L.; Nakashima, T. T.; Brown, D. W. *22nd Experimental NMR Conference*, 1981.

(3) Patt, S. L.; Shoolery, J. N. *J. Magn. Reson.* **1982**, *46*, 535-539.

(4) Lovenberg, W., Ed. "Iron Sulfur Proteins"; Academic Press: New York, 1973; Vol. II.

(5) Ho, K. K.; Ulrich, E. L.; Krogmann, D. W.; Gomez-Lojero, C. *Biochim. Biophys. Acta* **1979**, *545*, 236-248.

(6) London, R. E.; Kollman, V. H.; Matwiyoff, N. A. *J. Am. Chem. Soc.* **1975**, *97*, 3565-3573.

(7) Chan, T.-M.; Hermodson, M. A.; Markley, J. L.; unpublished results.

constants ( $\sim 7$ – $10$  Hz), the multiplicities of peaks in this region are either singlets (nonprotonated carbons) or doublets (singly protonated carbons) with coupling constants between 160 and 220 Hz. In the normal, single-pulse 50.31-MHz  $^{13}\text{C}$  NMR spectrum of oxidized ferredoxin shown in Figure 1a, the multiplicities are suppressed by on-resonance, broad-band  $^1\text{H}$  decoupling during spectral acquisition.

The APT pulse sequence used for Figure 1b was as follows: (delay,  $90^\circ$  pulse,  $\tau$ ,  $180^\circ$  pulse,  $\tau$ , acquisition) $_n$ , where the delay = 3.6 s,  $\tau$  = 6 ms,  $n$  = 3000. The square-wave-modulated<sup>8</sup> on-resonance decoupling was gated off during the first  $\tau$  and was on for the remainder of the pulse sequence; high-power decoupling (10 W) was used during the second  $\tau$  and acquisition, and low-power decoupling (2 W) was used at other times. The inverted peaks arise from carbons having a single attached proton, whereas the positive peaks arise from nonprotonated carbons. Transverse relaxation during the delay time ( $\tau$ ) employed in the APT pulse sequence results in some loss of intensity of the broader peaks in the spectrum. The APT spectrum of tryptophan, an amino acid not present in *A. variabilis* ferredoxin, is shown in Figure 1e.

A recent modification of the classic single-frequency off-resonance decoupling experiment,<sup>9</sup> which has been used to distinguish methine and nonprotonated aromatic carbons in proteins<sup>10</sup> as well as carbons affected differentially by long-range coupling,<sup>11</sup> is the spin-echo sequence with off-resonance broad-band decoupling.<sup>12</sup> The latter pulse sequence was used to obtain the spectrum in Figure 1c. Note that the peaks in this spectrum that arise from nonprotonated carbons correspond to the positive peaks in the APT spectrum.

For comparison purposes, Figure 1d shows a convolution difference spectrum.<sup>13</sup> This method, which is commonly used to resolve the sharper, nonprotonated carbons in  $^{13}\text{C}$  NMR spectra of proteins,<sup>10</sup> does not eliminate completely the residual broad components arising from protonated carbons and leads to artificial negative wings around peaks.<sup>13</sup>

Figure 2 illustrates a method of simplifying APT spectra. The sum of a normal single-pulse spectrum (Figure 2b) and an APT spectrum (Figure 2c) results in a subspectrum (Figure 2a) that contains resonances from only the nonprotonated carbons. The difference between the normal and APT spectra yields a subspectrum containing peaks of protonated carbons only (Figure 2d). This simplification is especially useful for interpreting the region around 130 ppm, where there is severe overlap of peaks from protonated and nonprotonated carbons. Some caution has to be used when making use of these sum and difference spectra because of the loss of intensity of APT peaks resulting from the time delay between pulses. For example, the peaks present around 115 ppm in Figure 2a represent artifacts. A broad-band-decoupled spin-echo spectrum with the delays set equal to those used in the APT sequence provides a better "normal" spectrum than a single-pulse spectrum for use in the sums and differences.<sup>14</sup>

Heteronuclear,  $J$ -resolved,  $^{13}\text{C}$  NMR spectroscopy provides an elegant method of determining the  $^1\text{H}$ - $^{13}\text{C}$  coupling pattern in small organic molecules.<sup>15</sup> The application of this technique to a protein is shown in Figure 3a, which displays a contour plot of a two-dimensional heteronuclear,  $J$ -resolved  $^{13}\text{C}$  NMR spectrum of oxidized *A. variabilis* ferredoxin. The  $^{13}\text{C}$  chemical shifts and coupling constants ( $^1J_{\text{H}-^{13}\text{C}}$ ) are separated into the horizontal and vertical axes, respectively. Nonprotonated carbons give rise to contours at  $J_{\text{C-H}}/2 = 0$  Hz. Protonated carbons yield a symmetrical pair of contours whose vertical separation is one-half the

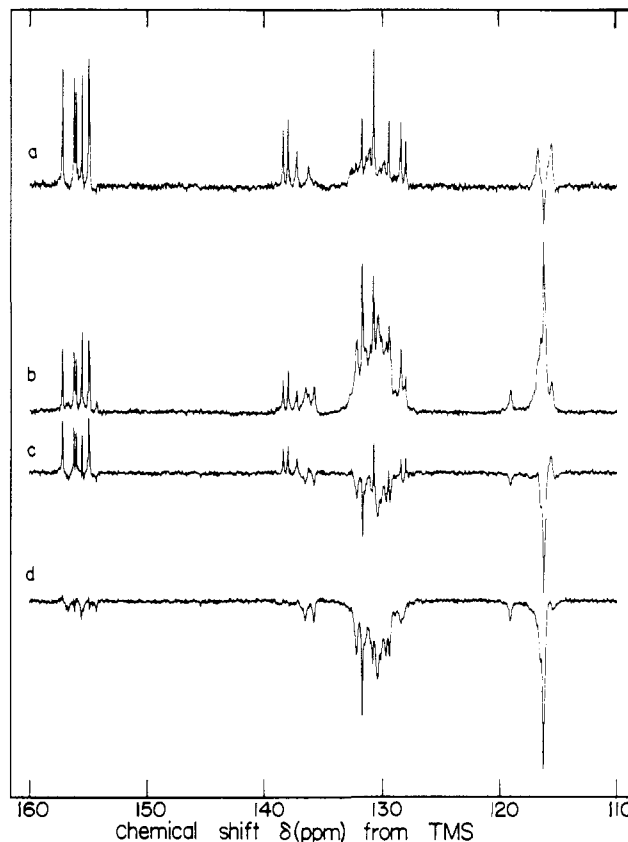


**Figure 2.** Generation of  $^{13}\text{C}$  NMR subspectra of the aromatic region of oxidized *A. variabilis* ferredoxin. Spectrum a, which is the sum of a normal single-pulse spectrum (spectrum b) and an APT spectrum (spectrum c), contains resonances from the nonprotonated carbons. Spectrum d, which is the difference between spectra b and c, contains resonances from the singly protonated carbons. Spectra b and c were obtained as described in Figure 1.

coupling constant ( $^1J_{\text{H}-^{13}\text{C}}$ ). An expansion of the APT spectrum is plotted in Figure 3b for comparison purposes. The doublets in the 128–134-ppm region all have coupling constants near 160 Hz. The two contour pairs near 136 ppm in the two-dimensional heteronuclear  $J$ -resolved spectrum that exhibit coupling constants of about 200 Hz are assigned to the  $\text{C}_\alpha$  ring carbons of the two histidine residues.<sup>16</sup> Since the other coupling constants are so uniform, they are not useful for assignment purposes. The main feature of the two-dimensional heteronuclear  $J$ -resolved spectrum

(16) Chan, T.-M.; Markley, J. L. *J. Am. Chem. Soc.*, following paper in this issue.

(17) All spectra were obtained with a Nicolet NT-200 NMR spectrometer using a spherical glass cell (Wilmad) inside a 20-mm o.d. NMR tube. Sample temperatures were 24  $^\circ\text{C}$ . Samples: spectra a–d, 6.5 mM oxidized *A. variabilis* ferredoxin in 50 mM phosphate buffer, pH 7.1, in  $^2\text{H}_2\text{O}$ ; spectrum e, 25 mM L-tryptophan in  $^2\text{H}_2\text{O}$ , pH 7.5. Spectrometer settings: 8K points digitized and zero filled to 32 K;  $90^\circ$  pulse = 28  $\mu\text{s}$ ; 4-s recycle time unless otherwise noted; two-level (10 W during acquisition, 2 W off acquisition unless otherwise noted) decoupling power:  $\pm 5500$ -Hz window with quadrature detection. Spectrum a: 2000 single  $90^\circ$  pulse acquisitions. Spectrum b: see text for details. Spectrum c: (delay,  $90^\circ$  pulse,  $\tau$ ,  $180^\circ$  pulse,  $\tau$ , acquisition) $_n$ , where delay = 3.6 s,  $\tau$  = 20 ms,  $n$  = 5000, square-wave-modulated decoupling 6000-Hz off-resonance at all times except during the delay. Spectrum d: data obtained by averaging 3000 single  $90^\circ$  pulse acquisitions; convolution difference spectrum obtained by subtracting a spectrum digitally broadened by 10 Hz from a spectrum digitally broadened by 1 Hz; off-resonance decoupling with the carrier placed 10 ppm upfield from  $(\text{CH}_3)_4\text{Si}$  and modulated over a band width of  $\pm 1350$  Hz; decoupler power 5 W during acquisition. Spectrum e: same conditions as spectrum b, except delay = 5 s; 14 000 acquisitions.

(18) Amplitude-modulated  $J$ -spectrum (spectrum 3a): ( $90^\circ$  pulse,  $\tau$ ,  $180^\circ$  pulse,  $\tau$ , acquisition) $_n$ , where  $n$  = 1200 and where  $\tau$  was incremented from 2 ms in 2-ms intervals to 128 ms for the second dimension; the decoupler was gated off during the second  $\tau$ . The sample contained 6.5 mM oxidized *A. variabilis* ferredoxin in 50 mM phosphate buffer, pH 7.0, 26  $^\circ\text{C}$ . The APT spectrum (Figure 3b) was obtained under slightly different conditions (pH 7.1, 24  $^\circ\text{C}$ ; see Figure 1), which explains the small difference in histidine chemical shifts.

(8) Grutzner, J. B.; Santini, R. E. *J. Magn. Reson.* **1975**, *19*, 173–187.

(9) Ernst, R. R. *J. Chem. Phys.* **1966**, *45*, 3845–3861.

(10) Allerhand, A.; Childers, R. F.; Oldfield, E. *Biochemistry* **1973**, *12*, 1335–1341.

(11) Oldfield, E.; Norton, R. S.; Allerhand, A. *J. Biol. Chem.* **1975**, *250*, 6381–6402.

(12) Opella, S. J.; Cross, T. A. *J. Magn. Reson.* **1980**, 171–175. Cookson, D. J.; Smith, B. E.; White, N. *J. Chem. Soc., Chem. Commun.* **1981**, 12–13.

(13) Campbell, I. D.; Dobson, C. M.; Williams, R. J. P.; Xavler, A. V. *J. Magn. Reson.* **1973**, *11*, 172–181.

(14) Westler, W. M.; Markley, J. L., unpublished results.

(15) Freeman, R.; Morris, G. A. *Bull. Magn. Reson.* **1979**, *1*, 5–26.

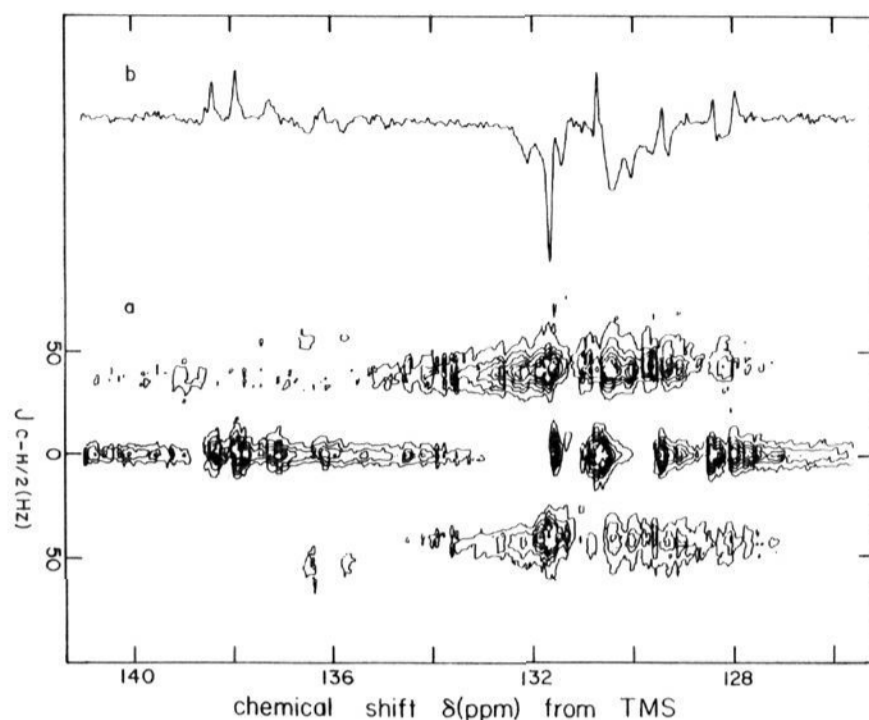


**Figure 3.** (a) Two-dimensional heteronuclear ( $^1\text{H}$ - $^{13}\text{C}$ )  $J$  spectrum<sup>15</sup> displayed as a contour plot.<sup>18</sup> The chemical shifts are displayed in ppm along the horizontal axis, and the coupling constants are given by twice the vertical separation between pairs of contour spots in Hz. (b) The APT spectrum<sup>2,3</sup> ( $^{13}\text{C}$  NMR  $J$ -modulated spin-echo experiment) is plotted for comparison.

is then the determination of spin multiplicity, but the APT sequence is competent for this purpose as well as being much less time consuming.

These results demonstrate that the APT pulse sequence provides an efficient method for determining the multiplicity of  $^{13}\text{C}$  NMR peaks in a small protein. The following communication<sup>16</sup> describes how extensive assignments of the subspectrum consisting of protonated carbons can be made by use of heteronuclear ( $^1\text{H}$ - $^{13}\text{C}$ ) two-dimensional correlation spectroscopy.

**Acknowledgment.** This work was supported by a grant from the Competitive Research Grants Office, CSRS, S & E, and USDA and by NIH grant RR 01077 from the Biotechnology Resources Branch of the Division of Research Resources. NMR spectroscopy was carried out in the Purdue Biochemical Magnetic Resonance Laboratory.

### Heteronuclear ( $^1\text{H}$ , $^{13}\text{C}$ ) Two-Dimensional Chemical Shift Correlation NMR Spectroscopy of a Protein. Ferredoxin from *Anabaena variabilis*

Tze-Ming Chan and John L. Markley\*

Department of Chemistry, Purdue University  
West Lafayette, Indiana 47907

Received February 8, 1982

Relatively few examples of extensive assignments in  $^{13}\text{C}$  NMR spectra of proteins are to be found in the literature. Allerhand and co-workers used the convolution difference technique to resolve resonances due to nonprotonated carbons in cytochrome *c* and lysozyme; in favorable cases, these peaks could be assigned to specific carbon atoms in the proteins.<sup>1</sup> Several  $^{13}\text{C}$  resonances due to methyl groups that have well-resolved  $^1\text{H}$  resonances were assigned by Wüthrich and co-workers in spectra of bovine pancreatic trypsin inhibitor by the use of single-frequency selective decoupling.<sup>2</sup> We report here the use of heteronuclear ( $^1\text{H}$ ,  $^{13}\text{C}$ ) two-dimensional (2-D) chemical shift correlation NMR<sup>3</sup> for the assignment of resonances from protonated carbons in proteins.

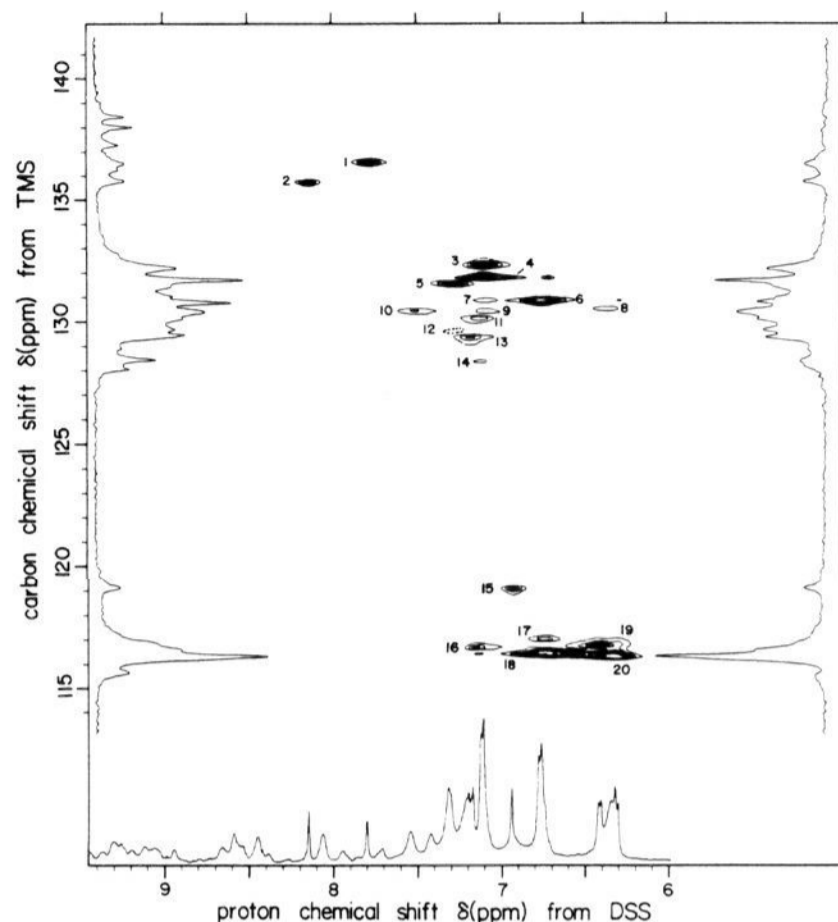


**Figure 1.** Cross assignment of chemical shifts in the  $^1\text{H}$  and  $^{13}\text{C}$  NMR spectra of the aromatic region of oxidized ferredoxin from *A. variabilis* by means of a heteronuclear two-dimensional chemical shift correlation map obtained at  $^{13}\text{C}$  and  $^1\text{H}$  resonance frequencies of 50.31 and 200 MHz, respectively, at 24 °C. A 470-MHz one-dimensional  $^1\text{H}$  NMR spectrum of the protein is shown at the bottom. Two 50.31-MHz one-dimensional  $^{13}\text{C}$  NMR spectra are plotted at the sides. That on the right-hand side is a subspectrum<sup>7</sup> that contains resonances from only protonated carbons, i.e., those expected to show up in the 2-D contour plot. The ferredoxin, which has two histidine, five tyrosine, and three phenylalanine residues, was enriched uniformly with  $^{13}\text{C}$  (20% level of isotope) to increase the signal-to-noise ratio. Contour peak 12 (dashed) was observed at a lower contour than the others shown.

Proton-carbon 2-D chemical shift correlation spectroscopy has been applied recently to small molecules<sup>4</sup> and to a series of carbohydrates.<sup>5</sup> The extension of this technique to proteins is hindered by the insensitivity of  $^{13}\text{C}$  NMR. However, this technique will be useful for small proteins or other macromolecules enriched in  $^{13}\text{C}$  or for small unenriched macromolecules that are very soluble and can be obtained in large quantity. The increase in time required is more than offset by the additional information gained.

It is easier, in general, to obtain assignments to specific residue positions for  $^1\text{H}$  than for  $^{13}\text{C}$  NMR spectra of proteins. Because of the high sensitivity of  $^1\text{H}$  NMR spectroscopy, several strategies can be used that may not be practical in  $^{13}\text{C}$  NMR spectroscopy, for example pH titrations and comparisons of spectra from proteins having homologous sequences. Two-dimensional chemical shift correlation allows the cross assignment of  $^1\text{H}$  and  $^{13}\text{C}$  NMR peaks from bonded pairs of  $^{13}\text{C}$ - $^1\text{H}$  nuclei. Also, better resolution can be achieved by spreading the resonances in two dimensions according to their proton and carbon chemical shifts. Resonances from protonated carbons in proteins can be grouped into two regions, the aliphatic region (from about 10 to 70 ppm from tetramethylsilane) and the aromatic region (110–140 ppm). The corresponding proton chemical shifts are similarly segregated. It is desirable to obtain separate 2-D correlation spectra for each region in order to allow better digital resolution in the proton chemical shift dimension.

The contour plot of a 2-D spectrum of the aromatic region of oxidized *Anabaena variabilis* ferredoxin is shown in Figure 1. The protein is a metalloprotein of  $M_r$  11 000 with a 2Fe-2S\* cluster;<sup>6</sup>

(1) Oldfield, E.; Norton, R. S.; Allerhand, A. *J. Biol. Chem.* **1975**, *250*, 6368–6380.

(2) Richarz, R.; Wüthrich, K. *Biochemistry* **1978**, *17*, 2263–2269.

(3) Maudsley, A. A.; Ernst, R. R. *Chem. Phys. Lett.* **1977**, *50*, 368–372.

Maudsley, A. A.; Müller, L.; Ernst, R. R. *J. Magn. Reson.* **1977**, *28*, 463–469.

(4) Freeman, R.; Morris, G. A. *Bull. Magn. Reson.* **1979**, *1*, 5–26.

(5) Morris, G. A.; Hall, L. D. *J. Am. Chem. Soc.* **1981**, *103*, 4703–4711.

(6) Hall, D. O.; Rao, K. K. In "Encyclopedia of Plant Physiology"; New Series; Springer-Verlag, New York, 1977; Vol. 5, p 206.